IEEE Access
Multidisciplinary | Rapid Review | Open Access Journal

Received April 19, 2018, accepted June 5, 2018, date of publication June 15, 2018, date of current version July 12, 2018.

Digital Object Identifier 10.1109/ACCESS.2018.2847732

Multi-Objective Optimum Design of High-Speed Backplane Connector Using Particle Swarm Optimization

WENJIE YU[1], ZHI ZENG[1,2], BEI PENG[1], SHUO YAN[1], YUESHUANG HUANG[1], HAI JIANG[1], XUNBO LI[1], AND TAO FAN[1]

[1]School of Mechatronics Engineering, University of Electronic Science and Technology of China, Chengdu 611731, China
[2]Institute of Electronic and the Information Engineering of UESTC in Guangdong, Guangdong 23808, China

Corresponding author: Zhi Zeng (zhizeng@uestc.edu.cn)

This work was supported in part by the Science and Technology Planning Project of Sichuan Province under Grant 2018GZ0284 and in part by the National Natural Science Foundation of China under Grant 51205047.

ABSTRACT This paper outlines a new procedure for computer modeling and optimum design for the dynamic mechanical and electrical study of a high-speed backplane connector, which is a key electrical interconnection technology in large communications equipment, ultra-high performance servers, supercomputers, industrial computers, high-end storage devices, and so on. The optimum structure design of contact pairs is important for a backplane connector in meeting multiple challenges in terms of minimizing the maximum insertion force and the contact resistance. Current optimization schemes, such as the quadrature method, are relatively complex. Therefore, we designed the connector contact pairs for simultaneously obtaining the proper insertion force and the contact resistance through a multi-objective particle swarm optimization (MCDPSO) method with simpler settings and faster convergence speed. In this paper, the required insertion force was minimized during the entire process, and the minimum contact resistance was maintained after insertion. To this end, an MCDPSO algorithm was proposed for the connector design. A dynamic weight coefficient was developed to calculate the interval values of the reserved solutions for the selection of the operator, and an external archive update based on roulette wheel selection and gbest selection strategies was developed to increase the diversity of the solutions. A set of optimal structure solutions of the contact pairs was obtained for the subsequent design optimization. The feasibility and effectiveness of the proposed method were verified by comparing with the results from ANSYS finite element simulation.

INDEX TERMS High-speed backplane connector, contact pairs, insertion force, contact resistance, multi-objective connector design, particle swarm optimization algorithm.

I. INTRODUCTION

A high-speed backplane is an important part of a modern inter-connection system, the performance of which is directly related to whether or not the entire system can function properly [1]. These backplanes are widely used in large communications equipment, ultra-high performance servers, super-computers, industrial computers and high-end storage devices. The connectors on these backplanes are the electrical interconnection mediation between the mother plane and the daughter plane [2], [3].

Among many properties of the backplane connector, the contact resistance and the insertion force are the two key factors that affect its mechanical and electrical properties. The contact resistance between the pins, which must be sufficiently small, depends on the normal force. The required normal force is a component of the contact force imposed by the contact pairs, which establishing the contact interface as mated is a key factor in determining the reliability of the backplane connector [4]. The stability of this low contact resistance between contact-containing components is critical to maintain proper operation of the electrical connector. A high contact normal force is desired for reducing the contact resistance. While the normal force on the contact interface is positively related to the insertion force, which is the most important mechanical characteristic of the electrical connector. There are strict requirements on the maximum

insertion force; low or zero-insertion-force (ZIF) connectors are much more popular due to their better performance and have been brought to the forefront for electrical contact reliability. Usually, several pins are assembled on the backplane connector, which may easily result in an associated increase of the insertion force. However, a large insertion force can cause problems in assembly and in other parts of the electronic devices. In summary, the contact force plays an important role in the contact resistance and the insertion force at the same time. Normally, the dimensions, environmental factors (including temperature and vibration), etc., can impact the contact force. Among these influencing factors, structural parameters are most important [5]–[7]. Therefore, the optimal design of the contact pairs is necessary to achieve both the required low insertion force and low contact resistance.

In the literature, some researchers have analyzed the contact force of electronic connectors [8]–[11]. Li *et al.* [12] investigated the insertion force and contact reliability of an N-type electric connector with a finite element model (FEM). El Manfalouti *et al.* [13] presented a new experimental method based on a laser technique for non-intrusive probing of the deflection of the spring terminal to determine the connector parameters during insertion and extraction. Yeh-Liang Hsu et al. converted multi-objective optimization to a single target and used a sequential linear programming algorithm to solve it. These studies paid much attention on the mechanical objectives optimization using traditional methods. While, few approaches focus on the mechanical and electrical objectives (like contact resistance optimization) simultaneously by numerical methods.

Compared to the experimental method and finite element simulation, numerical optimization methods are more efficient in engineering [14], [15]. The problem we studied contains multiple parameters to adjust and two objectives to accomplish: minimum insertion force and minimum contact resistance, which is called a multi-objective optimization problem (MOP). Several traditional algorithms (constraint method, linear weighted method, minimax method, etc.) and evolutionary algorithms (Multi-Objective Genetic Algorithm (MOGA) [16], Multi-Objective Evolutionary Algorithm Through Decomposition (MOEA/D) [17], Multi-objective Particle Swarm Optimization (MOPSO) [18], etc.) have been developed to solve this type of problem. After in-depth study of this issue, intelligent multi-objective optimization algorithms are increasingly favored by many scholars and experts because of their increasing solution accuracy. In recent years, multi-objective particle swarm optimization has been developed rapidly [19]–[23]. Compared to MOGA, MOPSO searches faster, while its use in practice is much simpler, and it can also be used for most engineering problems; hence it has become a research hotspot and been applied widely in many engineering fields [24]–[29]. Nevertheless, its optimal results are still not sufficiently accurate for the test functions, and the diversity of the designed parameters is not uniform [30]. Several researchers have put forward some improved multi-objective particle swarm optimization algorithms. However, the global and local search abilities of these algorithms need to be further balanced, and the diversity of the solution set of these algorithms is not adequately helpful [31]. In the proposed approach, we developed a multi-objective particle-swarm optimization algorithm (MCDPSO) for the optimal design of contact pairs for high-speed backplane connectors. In MCDPSO, a dynamic weight coefficient was used to avoid falling into local optimums thus improve the accuracy of structure parameters for the design of contact pairs. Additionally, we proposed the external archive updates based on roulette-wheel selection and *gbest* selection strategies to improve the diversity of the algorithm to obtain more non-dominated parameter vectors for contact-pair design.

- Aimed at optimizing the contact resistance and the insertion force of the backplane connector simultaneously, an improved multi-objective method, MCDPSO, is developed to tackle this problem via optimum design of the backplane connector structural parameters. Our contribution can be summarized as follows:
- A mechanical model of a contact pair was built based on an approximate differential model of the deflection of beams and on electrical contact theory. The optimization model was developed according to the requirements to have both a low insertion force and low contact resistance.
- An improved MOPSO was developed, MCDPSO, to solve this model. To verify the effectiveness of this algorithm, we used an efficient set spacing metric and a two-set coverage metric to compare the results with a real engineering instance and MOPSO. Additionally, the results based on ANSYS Workbench simulation were compared with the numerical results and a discussion from mechanical view was given.

II. A MECHANICAL MODEL OF CONTACT PAIRS AND PROBLEM FORMULATION

A. STRUCTURE OF CONTACT PAIRS IN A CONNECTOR

Usually, there are several contact pairs in a high-speed backplane connector (as shown in Fig. 1(a), (b)). A contact pair is illustrated in Fig. 1(c); it is composed of pin A, pin B and the base. Pin A is a double cantilever beam, and pin B is a single cantilever beam. In this investigation, pin A is inserted into the base firstly, and then the mating process of pin B is analyzed by a dynamic model.

B. MECHANICAL MODEL OF INSERTION FORCE

As mentioned above, the structure of the electric connector has a great influence on the insertion force and contact resistance; the simplified model of the insertion process mainly considered the structure, while the speed of insertion, temperature, vibration and other factors were ignored in this study.

The insertion process is shown in Fig. 2(a). When pin B is inserted between pin A and the base, pin A experiences an elastic deformation, resulting in a normal force of the contact interface to generate contact resistance. The insertion mating process can be divided into the following three stages:

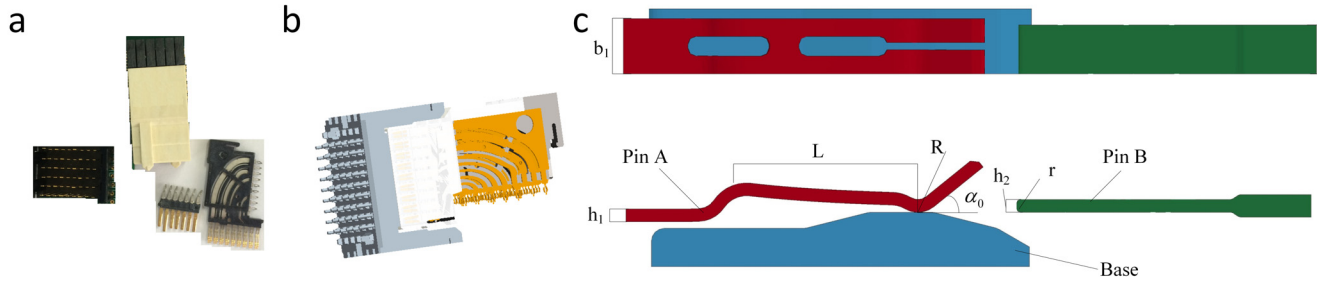

FIGURE 1. Structure of a high-speed backplane connector: a. high speed backplane connectors. b. CAE model. c. contact pair: Pin A length, width and thickness are L, b_1 and h_1, respectively. R and α_0 are the pin A bending radius and starting angle with the base.h_2 and r are the thickness and chamfer radius of pin B.

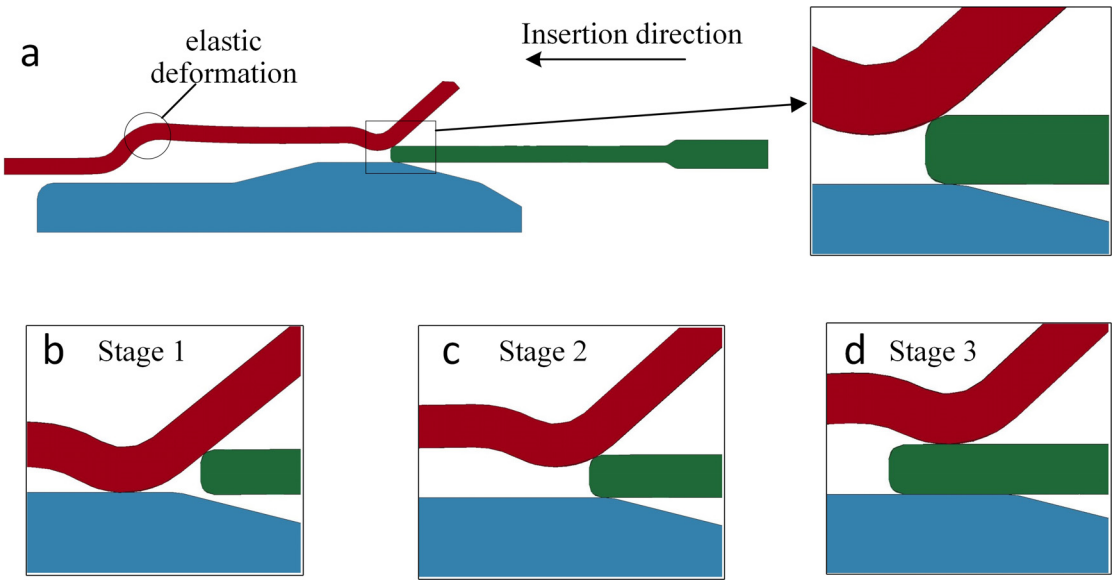

FIGURE 2. Insertion process of the contact pair: a. insertion process b. Stage 1. c. Stage 2. d. Stage 3

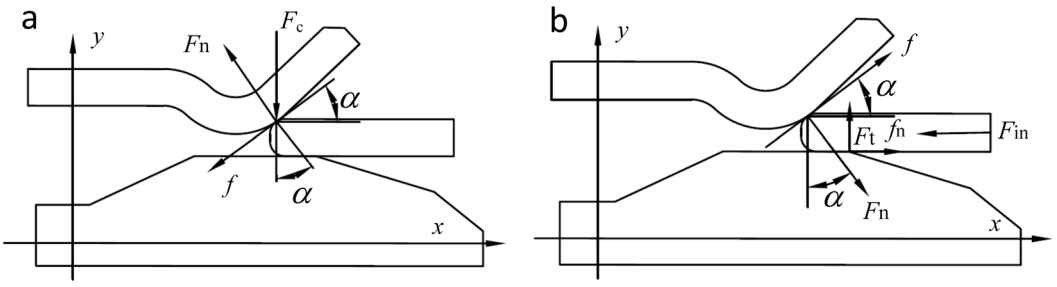

FIGURE 3. Force analysis of contact pair: a. Force analysis of pin A b. Force analysis of pin B.

- Stage 1. The fillet surface of pin B contacts the inclined plane of pin A.
- Stage 2. The fillet surface of pin B contacts the circular arc surface of pin A.
- Stage 3. The upper plane of pin B contacts the circular arc surface of pin A.

Diagrams of stages 1-3 are shown in Figs. 2(b), (c) and (d).

The force diagram in the insertion process is shown in Fig. 3, where F_c is the contact force, α is the contact pressure angle, f is the friction between pins, f_n is the friction between pin B and the base, F_t is the supporting force, and $\mu$is the coefficient of friction between the contact surfaces. The relationship equation between the contact pressure generated by the elastic deformation of pin A and the insertion force is

expressed as follows:

$$F_{\text{in}} = \mu F_c + \frac{F_c(\mu + \tan\alpha)}{1 - \mu\tan\alpha} \tag{1}$$

Pin A can be simplified as a cantilever beam with a variable cross section. The approximate differential equation of the deflection of beams is:

$$y'' = -\frac{M(s)}{EI(s)}. \tag{2}$$

where $M(s)$ is the bending moment expression, E is the elastic modulus and $I(s)$ is the cross-sectional moment of inertia expression.

The chamfer of pin A (at the slot division) has little effect on the result. To simplify the calculation, the chamfer is ignored here. The expressions $M(s)$ and $I(s)$ of pin A are:

$$M(s) = F_c(L - s) \tag{3}$$

$$I(s) = \begin{cases} \frac{1}{12}h_1^3(b_1 - 0.3), & (0 \le s < 0.88 \& 1.45 \le s < 2.70) \\ \frac{1}{12}h_1^3 b_1, & (0.88 \le s < 1.45) \\ \frac{1}{12}h_1^3(b_1 - 0.06), & (2.70 \le s \le L) \end{cases} \tag{4}$$

Integrating (2) over s twice, the deflection equation can be expressed as:

$$y = \int [\int -\frac{M(s)}{EI(s)}ds]ds + Cs + D \tag{5}$$

Substituting (3), (4) and the deflection δ into (5), the contact force F_c can be expressed as:

$$F_c = k\frac{E\delta h_1^3}{12K} \tag{6}$$

where k is a correction factor and

$$K = \frac{[5.13L^2 - b_1(50L^3 - 238.5L^2 - 669) \\ -11.95L + 166.67L^3 b_1^2 + 7.1]}{b_1(10b_1 - 3)(50b_1 - 3)} \tag{7}$$

Due to the change of the constant-pressure angle and the deflection in the process of insertion, it is necessary to know the change of the pressure angle over the insertion distance.

1) Stage 1
In this stage, the pressure angle $\alpha = \alpha_0$, and the deflection $\delta = (s - s_0)\tan\alpha_0$, where s is the insertion distance and s_0 is the insertion position of initial contact.
2) Stage 2
The contact in this stage is two round surfaces in contact as shown in Fig. 4. During this process, α can be obtained as follows:

$$\alpha = \arcsin(\alpha_0 - \frac{\Delta s}{R + r}) \tag{8}$$

$$\Delta s = s - s_1 \tag{9}$$

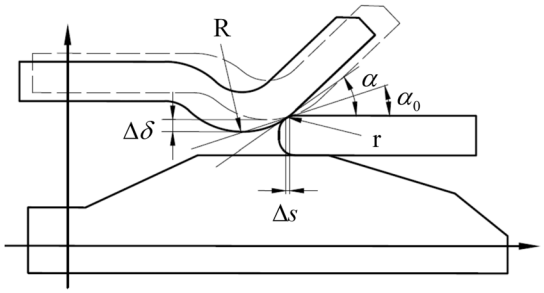

FIGURE 4. Schematic diagram of the mating process.

where s_1 is the insertion distance at the end of stage 1. From Fig. 4, the deflection δ can be obtained by writing the relationship between δ and α.

$$\Delta\delta = (r + R)(\cos\alpha - \cos\alpha_0) \tag{10}$$

$$\delta = \delta_1 + \Delta\delta \tag{11}$$

where δ_1 is the deflection at end of stage 1.

3) Stage 3
As the insertion distance increases, the pressure angle decreases, finally becoming s_0, and the deflection is equal to h_2.

C. MECHANICAL MODEL OF CONTACT RESISTANCE

Because the true contact area is smaller than the apparent area in contact, it is assumed that the true contact area is determined by plastic deformations of the asperities projecting from the surfaces. The relationship between the area of mechanical contact and the contact force is given by [32]:

$$F_n = HA_C \tag{12}$$

where H is the material hardness, F_c is the normal pressure, which according to Fig. 3 can be deduced as:

$$F_c = F_n \cdot \cos\alpha - f \cdot \sin\alpha \tag{13}$$

And A_C is the true area of contact. The true area of contact can be written as:

$$A_C = \pi\beta^2 \tag{14}$$

where β is the constriction radius. Equation (12) can be rewritten as:

$$\beta = \left[F_n/(\pi H)\right]^{\frac{1}{2}} \tag{15}$$

In addition, the contact resistance R_C can be given by [33]

$$R_C = \rho/(2\beta) \tag{16}$$

where ρ is the electrical resistivity. Using (14) and (15), the following can be deduced:

$$R_C = (\rho/2)[\pi H/F_n]^{1/2} \tag{17}$$

D. PROBLEM FORMULATION

For a contact pair of a high-speed backplane connector, the insertion force is the dynamic quantity that varies with the insertion distance s. The maximum insertion force should be as small as possible, while the contact resistance should be minimized during stage 3 of the insertion process. In this investigation, $b_1, h_1, R, \alpha_0, h_2$ and r were selected as the decision variables based on the engineering practice. The values of these decision variables were limited to a certain extent derived by engineering design experiments. The specific values are given in the subsection IV-B. The optimization model of this contact is expressed as follows:

$$\begin{cases} \min \max\limits_{s} F_{\text{in}}(x, s) \\ \min R_C \\ x = (b_1\ h_1\ \alpha_0\ h_2\ R\ r) \\ \text{s.t. } \Phi \le x \le \Gamma \end{cases} \tag{18}$$

where Φ and Γ denote the lower and upper limits of the decision variables, respectively.

In this problem formulation, the insertion force F_{in} and the contact resistance R_c are the two objectives needed to be optimized simultaneously. As can be seen from (1), the insertion force is in direct proportion to the contact force F_c. By using (13) and (17) the contact resistance R_c can be rewritten as:

$$R_C = (\rho/2)[\pi H(\cos\alpha - \mu \sin\alpha)/F_c]^{1/2} \tag{19}$$

which is inversely proportional to the contact force F_c. Obviously, the insertion force F_{in} and the contact resistance R_c change in opposite ways when the pressure angle α changes slightly. Therefore, this is a multi-objective optimization problem.

III. OPTIMUM MULTI-OBJECTIVE DESIGN METHODS FOR CONNECTOR CONTACT PAIRS

In this section, we will introduce the MCDPSO method. As already noted, the method is based on PSO [34] in a multi-objective setting. First, we depict the strategy of combining PSO with the multi-objective optimization. Then, we present a particle representation and objective functions for the contact-pair design. Finally, we give a detailed presentation of MCDPSO conceived for the optimum design of high-speed backplane connector contact pairs.

A. MULTI-OBJECTIVE PARTICLE SWARM OPTIMIZATION

In PSO, each particle in a set of particles flies to an optimal location relative to its own previous best position (*pbest*) and the best neighborhood particle's position (*gbest*). The position and velocity of the ith particle are expressed as x_i and v_i. The position and velocity are updated as follows:

$$x_i^{t+1} = x^t + v_i^t \tag{20}$$

$$v_i^{t+1} = \omega v_i^t + c_1 r_1 (pbest_i^t - x_i^t) + c_2 r_2 (gbest_i^t - x_i^t) \tag{21}$$

where t is the iteration number, ω is an inertial weight, c_1 and c_2 are acceleration coefficients, and r_1 and r_2 are two random numbers uniformly distributed between 0 and 1.

The original form of PSO is not capable of addressing multi-objective optimization problems. However, several recent approaches have extended the basic concept of PSO to solve such problems (MOPSO) [35]. These MOPSO studies employed the concept of Pareto optimality to choose non-dominated particles in the population as leaders and let solutions converge to the true Pareto front [35]. In such multi-objective problems, each particle may have a set of different leaders of which just one is chosen for the position updating. The leaders (non-dominated solutions) found during the optimization process are usually saved in a repository called an external archive. These saved non-dominated solutions are employed as leaders when particle positions must be updated in the search space. In particular, all particles contained in the external archive are usually assumed as the final Pareto optimal solutions obtained by the algorithm.

B. PARTICLE REPRESENTATION AND OBJECTIVE FUNCTIONS FOR DESIGN OF A CONTACT PAIR

With the objective of applying MCDPSO to optimum design of contact pairs, a reasonable representation of particles for each set of contact pair structure parameters needs to be set firstly. In this approach, each particle x is represented by a vector composed of multi-dimensional contact-pair parameters, i.e.,$x = (b_1, h_1, \alpha_0, h_2, R, r)$. Because every structure parameter is continuous, the combination of any two positions is a continuous operation. Note that the particles may occasionally fly to positions beyond the defined search space, hence produce invalid solutions. To prevent this situation, some researchers have suggested some methods such as absorbing, reflecting and invisible walls. Huang and Mohan [36] proposed a damping wall, which has been verified to have robust and consistent optimization performance, regardless of the dimensionality and the location of the global optimum solution. Thus, a damping wall was selected for our approach.

The problem we studied has two objectives: insertion force F_{in} and contact resistance R_c. Once every particle has been set, these two objectives can be respectively calculated by (1) and (17).

C. MULTI-OBJECTIVE CONNECTOR DESIGN PARTICLE-SWARM OPTIMIZATION

The proposed MCDPSO algorithm is discussed in more detail in this section. It is a combinational form of the PSO algorithm within a multi-objective structure that combines some special features for optimum design of high-speed backplane connectors. The features are as follows.

1) DYNAMIC INERTIA WEIGHT

A large inertia weight helps to improve the global search ability of the algorithm, while a small inertia weight can enhance local searching. To prevent premature convergence and oscillation near the optimal solution as the algorithm terminates, a nonlinear decreasing inertial weight was employed

for iteration k:

$$\omega_k = \frac{\omega_{\max} - \omega_{\min}}{2} \times \left(\cos(\frac{\pi k}{T}) + 1\right) + \omega_{\min} \quad (22)$$

where ω_{max} and ω_{min} represent the maximum and minimum of the inertia weight, respectively, and T is the maximum number of iterations.

2) MAINTENANCE OF EXTERNAL ARCHIVE

The external archive consists of the position, fitness and crowding distance of the non-dominated solutions. Updating of the non-dominated solution set is based on Pareto dominance, and if there is no Pareto dominance between the two particles, one of them will be selected randomly. If there are multiple particles with the same information, only one will be kept in the external archive.

A fixed number n_{max} is set to control the size of the external archive $S_{archive}$. If the particles with only large crowding distances are retained, all other particles will be removed, which may reduce the diversity of the solutions [30]. For the electrical device design, especially for such a complex connector with many crucial elements, the optimized structural sizes would be expected to be uniform rather than focused on a limited section. Furthermore, the diversity of the solution is also a key criterion for the multi-objective optimization. Thus, when the contents of the external archive exceed the fixed number, some particles will be removed by the roulette wheel selection scheme [37], which is used to ensure the solution diversity of $S_{archive}$ and so as to avoid the algorithm falling into a local optimum. The pseudopod of external archive update is shown in Algorithm 1.

Algorithm 1 External Archive Update

Input a new solution setP_{new}.
1. outer: **for** each $p \in P_{new}$
2. insider: **for** each $p' \in P_{new} \& p' \neq p$
3. **if** p dominates p'
4. delete p' from P_{new}
5. **else if** p' dominates p
6. delete p from P_{new}
7. break out of the insider loop
8. **end if**
9. **end for**
10. **end for**
11. $S_{archive} = S_{archive} \cup P_{new}$
12. sort $S_{archive}$ based on crowding distance [38]
13. set $n_{over} = |S_{archive}| - n_{max}\ \%|S_{archive}|$ as the size of $S_{archive}$
14. **if**$n_{over} > 0$
15. use roulette wheel selection [37] to delete n_{over} elements from $S_{archive}$
16. **end if**

Output $S_{archive}$.

3) ELITIST SELECTION

Optimal position and global optimal position are the goals of the PSO particles. These points are tracked by the particles to optimize each iteration. PSO in its original form is single-objective. Selecting of *gbest* and *pbest* is simple and their values are unique. However, in MOPSO, many feasible solutions exist that cannot be distinguished by fitness. The method for selecting is the key to approaching the optimal boundary. Choosing *pbest* is easy and most common. Recent research focuses on Pareto-based dominance [39] which adopts a non-dominated particle between its current position and previous best position as the *pbest*. If one does not dominate, then pick one randomly. This scheme was adopted to handle *pbest* in our study.

The selection of *gbest* is relatively complex. Research in this area is in the following categories.

- Stochastic selection [40]. Random picking is used for non-dominant solutions saved in the external archive. However, when particles become concentrated, they are prone to have a greater probability of selection. This is not conductive to distribution along the optimal front and the diversity of the population.
- Crowding density [38]. Choose a particle as *gbest* with the minimum Euclidean distance between current particles and non-inferior solutions in the external archive.

In our approach, *gbest* was selected by Algorithm 2. The particle with the smallest ranking value has dominance and distribution. Choosing it as the *gbest* can speed convergence but may also reduce the diversity of the population and result in a local optimum trap of the algorithm. To avoid this, in Algorithm 2, the particle with smallest ranking value will have the highest probability of being chosen, while those with larger ranking values may still have some chance to be chosen. Specifically, we need to select one solution s_k from $S_{archive}$ as the *gbest* solution. The elements in $S_{archive}$ are sorted based on crowding distance. If we just pick the first element in $S_{archive}$, this may harm the diversity of the swarm. Thus, we generate the probability range (r^l, r^u) for each element in $S_{archive}$ according to its rank order, as depicted in line 5. r^l is the reachable lower bound of the range and r^u is the unreachable higher bound of the range. This means the best element has a great chance to win, but it is not absolute.

4) PSEUDOCODE OF MCDPSO

Based on the above methods, the pseudo-code of the MCDPSO is expressed as follows:

IV. EXPERIMENTAL RESULTS AND DISCUSSION

In this section, we evaluate the performance of MCDPSO. After a preliminary discussion of the MCDPSO parameters, we compare the performance of the proposed algorithm with MOPSO for some well-known benchmarks and for the optimum structure design of a high-speed backplane connector.

Algorithm 2 *gbest* Selection

Input a new solution set P_{new}.

1. generate a random number *rand*
2. set $i=1$, $k=0$
3. let $len = |S_{archive}|$ % $|S_{archive}|$ be the size of $S_{archive}$
4. **while** $i \leq len$
5. generate $[r_i^l, r_i^u)$ for $s_i \in S_{archive}$,

$$r_i^l = \frac{(i-1)(2len-i+2)}{len(len+1)}, \quad r_i^u = \frac{i(2len-i+1)}{len(len+1)}$$

6. **if** $rand \geq r_i^l$ & $rand < r_i^u$
7. $k = i$
8. break this loop
9. **end if**
10. $i = i+1$
11. **end while**

Output s_k as the *gbest* solution.

Algorithm 3 MCDPSO

1. Initialize
2. **for** each particle in swarm
3. generate the position and velocity randomly
4. update the velocity and position ((20) and (21))
5. evaluate
6. update *pbest*
7. **end for**
8. update external archive via Algorithm 1
9. obtain *gbest* via Algorithm 2
10. while (not-stopping criterion)
11. **for** each particle in swarm
12. update the velocity and position ((20) and (21))
13. evaluate
14. update *pbest*
15. **end for**
16. update external archive via Algorithm 1
17. obtain *gbest* via Algorithm 2
18. **end while**

Output external archive.

A. PERFORMANCE VALIDITY MEASURES

In this investigation, some strategies were employed in MCDPSO to strengthen its ability to find the optimum structure design of a high-speed backplane connector. To evaluate MCDPSO comprehensively, we employed a two-set coverage metric and a spacing metric to further rate the performance of MCDPSO on the connector structure design. The two-set coverage metric is defined as the percentage of the solutions in B that are dominated by at least one solution in A.

C(A, B) plus C(B, A) is not necessarily equal to 1. C(A, B) = 0 means that no solution in B is weakly dominated by any solution in A, while C(A, B)= 1 expresses that all solutions in B are weakly dominated by solutions in A [41].

The spacing metric [42] is used to assess the distribution of vectors throughout the set of non-dominated solutions. This metric is defined as the following:

$$S = \sqrt{\frac{1}{n-1}\sum_{i=1}^{n}\left(\bar{d}-d_i\right)^2} \tag{23}$$

where $d_i = \min_j \left(\left|f_1^i(x) - f_1^j(x)\right| + \left|f_2^i(x) - f_2^j(x)\right|\right), i, j = 1, \cdots, n$. A value of zero for this metric means that all vectors in the non-dominated solutions set are equidistantly spaced.

Note that for comparing these two algorithms on the connector structure design, the spacing metric was employed as the diversity metric because the true Pareto solutions of the problem of connector design are unknown.

B. PARAMETER SETTINGS

The materials of the backplane connector contact pairs in this approach is Cu0.98Be0.02. The material hardness H is 220N/mm^2 and its electrical resistivity value is $8.2\times10^{-5}\Omega \cdot$ m. We assumed some parameter values in our study. The lower and upper limits of the decision variables Φ and Γ were (0.8 0.18 35 0.18 0.3 0.04) and (0.9 0.23 45 0.23 0.5 0.09), respectively. The value of the coefficient of friction μ was 0.18. The correction factor k was as follows:

$$k = \begin{cases} 0.9 + \dfrac{0.3(s-s_0)}{s_0-s_2}, & s \leq s_2 \\ 0.6, & s > s_2 \end{cases} \tag{24}$$

where s_0 is the insertion distance of initial contact and s_2 is the insertion distance when stage 2 ended.

MCDPSO was applied to optimize the contact model compared with MOPSO. The parameters involved in these two algorithms include inertia weight (ω), population size (Popsize), cognitive parameter (c_1), social parameter (c_2), ran-dom values(r_1 and r_2), maximum iterations(*Maxcycle*) and the maximum external archive size(n_{max}). The parameters Popsize, c_1, c_2, r_1, r_2, *MaxCyble*, n_{max}, were set the same for both MOPSO and MCDPSO, but different in ω. As for the inertia weight factor, it is a constant (with the value 0.4 [40]) in MOPSO, and it is a dynamic changing value in MCDPSO. In MCDPSO, the maximum value for the inertia weight factor, $\omega_{\max}$, has been typically set to 0.9, for its ability to quickly foster the finding of a global optimum. The value ω_k is decreased until $\omega_{\min}$=0.4, to progressively turn the behavior of the algorithm from mainly exploratory (i.e. ω_k=0.9) to mainly exploitative (i.e. ω_k =0.4) [43].

As for the cognitive parameter and social parameter, according to the reference [44], the following parameter selection heuristic can be derived:

$$0 < (c_1 + c_2) < 4 \tag{25}$$

Generally, in order to guarantee the search balance of the algorithm, the acceleration constants c_1, c_2 are set to 2.0 [45]. The values of these parameters are shown in Table 1. To minimize the influence of random effects, the experiment was repeated 30 times for this problem, each time a different randomly generated initial population was used. First, the results

TABLE 1. Algorithm parameters.

Parameter	Description	Value
Popsize	Population size	60
ω	The inertia weight	0.4
ω_{min}	Minimum value of the inertia weight factor	0.4
ω_{max}	Maximum value of the inertia weight factor	0.9
c_1	Cognitive parameter	2
c_2	Social parameter	2
r_1	Random value	[0,1]
r_2	Random value	[0,1]
MaxCycle	Maximum iterations	3000
n_{max}	Maximum external archive size	100

of 30 independent runs were ranked according to the two-set coverage metric. Then, the median results of 30 independent runs were kept. The median results selected were employed to represent the general level of the algorithm, so as to avoid the extreme solutions sets. The MCDPSO algorithms and optimization calculations were implemented by MATLAB software.

C. PERFORMANCE EVALUATION OF MCDPSO ON CONNECTOR CONTACT PAIRS OPTIMUM DESIGN

In practice, high-speed backplane connector contact pairs are designed by the classic methods such as the quadrature method. A contact pair of a real connector has a structure parameters vector ($b_1 = 0.85$mm, h_1=0.2mm, $\alpha_0 = 37°$, $h_2 = 0.2$mm, $R = 0.4$mm, $r = 0.06$mm). Based on the mathematical model of contact pairs of section II, the maximum insertion force and contact resistance obtained were 0.358N and 1.55$m\Omega$, respectively. This connector's structure was designed by the quadrature method. In this study, multi-objective optimization strategies were employed to redesign this connector structure to achieve a smaller maximum insertion force and a lower contact resistance.

MOPSO is capable of achieving better solutions than the original connector design, as expressed in Fig. 5. This implies that multi-objective optimization methods can achieve good performance for this problem. However, the distribution of MOPSO solutions in Fig. 5 is not uniform, indicating the poor diversity of MOPSO. However, MCDPSO conceived with some modification strategies can improve the diversity, as shown in Fig. 6. Intuitively, the solutions obtained by MCDPSO distribute more uniformly, which means MCDPSO has better diversity performance than MOPSO. This can be verified by comparing MCDPSO and MOPSO with the spacing metric. The results are shown in Table 2. The value obtained by MCDPSO is smaller than those of MOPSO, indicating that MCDPSO has a better distribution of the obtained solutions set than MOPSO does.

TABLE 2. Results of the spacing metric for both algorithms.

S	MCDPSO	MOPSO
Average	0.01317	0.02014
Median	0.01262	0.01630
Std. Dev.	0.00177	0.00962

TABLE 3. Results of the coverage metric for the problem where A denotes MCDPSO and B denotes basic MOPSO.

C	*C* (A,B)	*C* (B,A)
Average	0.58454	0.53557
Median	0.57376	0.54399
Std. Dev.	0.08163	0.08619

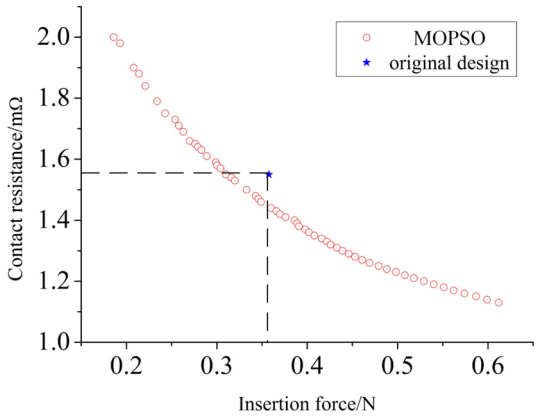

FIGURE 5. Non-dominated solutions by MOPSO.

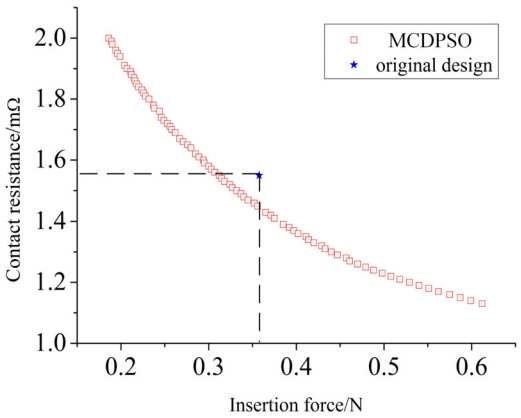

FIGURE 6. Non-dominated solutions by MCDPSO.

Furthermore, it can be observed from Figs. 5 and 6 that MCDPSO provides more feasible solutions. In a direct comparison based on the coverage metric, the results are given in Table 3. The value of MCDPSO is smaller, meaning that its average performance is slightly better. The solutions are

TABLE 4. Some optimal solutions better than original design.

Number	1	2	3	4	5	6	7	8
b_1/mm	0.877	0.875	0.879	0.861	0.862	0.867	0.869	0.872
h_1/mm	0.206	0.207	0.207	0.211	0.211	0.212	0.212	0.213
α_0/°	35.01	35.00	35.00	35.01	35.22	35.00	35.05	35.00
h_2/mm	0.180	0.180	0.180	0.180	0.180	0.180	0.180	0.180
R/mm	0.500	0.500	0.499	0.500	0.497	0.500	0.500	0.499
r/mm	0.090	0.090	0.090	0.090	0.087	0.090	0.089	0.090
maxF_{in}/N	0.318	0.324	0.327	0.332	0.337	0.34	0.345	0.352
R_C/mΩ	1.53	1.52	1.51	1.5	1.49	1.48	1.47	1.46

found better than the original design, as shown in Table 4. As shown in Table 4, the values of Pin B thickness h_2, bending radius R and Pin B chamfer radius r were kept constant while other parameters changed significantly. For subsequent optimization design, designers can fix the structural parameters h_2, R, and r and change other structural parameters to improve performance.

It can be observed that both MOPSO and MCDPSO work better than the original design in terms of the insertion force and contact resistance. MCDPSO can obtain more feasible solutions due to the dynamic inertia weight and also improve the diversity of the solution set distribution because of the external archive and *gbest* update strategies. The uniform optimal solution could also be obtained accordingly.

D. VERIFICATION OF NUMERICAL METHODS BASED ON ANSYS FINITE ELEMENT SIMULATION

In the previous subsection, MOPSO and MCDPSO have been used to obtain the structural parameters with the objective of optimizing the contact resistance and insertion force of the connector contact pairs. These results have been compared with those by classic methods. Regarding the solutions set coverage and diversity, MCDPSO showed a better performance than MOPSO for the optimization problem. The optimization results obtained by MOPSO and MCDPSO was further verified from the perspective of the mechanical structure via ANSYS simulation.

Firstly, software Soliworks 2016 was used to build the contact pair model of the backplane connector. This model is shown in Fig. 7. Then, the model constructed by Soliworks was imported into ANSYS Workbench R17.2 for mechanical analysis of the mechanical structure. In ANSYS, the application of constraints is shown in Fig. 8. Afterwards, the mechanical properties of the insertion process were analyzed. Mesh independence was verified in the simulation procedure.

For each set of the parameters obtained by MOPSO and MCDPSO, the maximum insertion force and the minimum contact resistance of the contact pair can be obtained through the simulation process of the pin process using ANSYS. Detailed results are shown in Tables 5 and 6. In these tables, the term "Number" corresponds to the same term in Table 4. The maximum insertion force and the minimum contact resistance obtained at the maximum insertion force obtained by multi-objective numerical methods and ANSYS simulation are given. The differences between the results of multi-objective numerical methods and ANSYS simulation results are given in the tables.

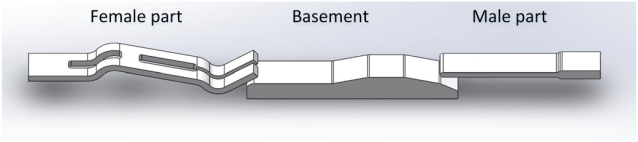

FIGURE 7. Connector contact pair model built by Soliworks 2016.

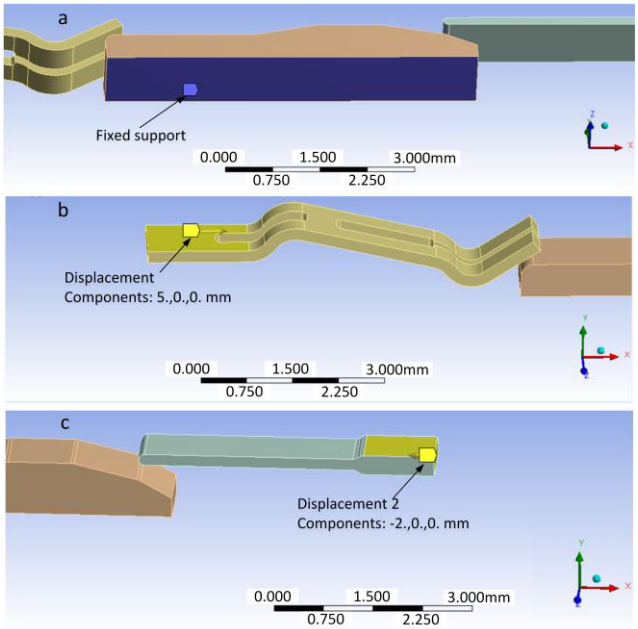

FIGURE 8. Constraints setting: a. Fix constraint imposing on basement. b. Displacement constraint on the Female side. c. Displacement constraint on the Male side.

The average differences among the simulation results among MOPSO, MCDPSO and ANSYS are given in Table 7. It can be seen that, for the average insertion force difference $\overline{\Delta F_{in}}$, the MCDPSO calculation result is closer to ANSYS simulation results than MOPSO. For the average contact resistance difference $\overline{\Delta R_c}$, the MOPSO calculation result is slightly better than MCDPSO. The differences between the multi-objective optimization result and the ANSYS simulation result are small, indicating that the result of the multi-objective optimization algorithm has certain

TABLE 5. Results comparison between MOPSO and ANSYS simulations.

Methods	Number	1	2	3	4	5	6
Results obtained by MOPSO	max(Fin)/N	0.3220	0.3350	0.3410	0.3470	0.3550	0.3560
	$R_c^{F_{in}=\max(F_{in})}$ / mΩ	1.530	1.500	1.490	1.488	1.460	1.450
Results obtained by ANSYS simulation	max(Fin)/N	0.3482	0.3728	0.3691	0.3904	0.3923	0.4039
	$R_c^{F_{in}=\max(F_{in})}$ / mΩ	1.526	1.544	1.483	1.438	1.464	1.463
Differences between the two methods	ΔF_{in}	7.52%	10.14%	7.61%	11.12%	9.51%	11.86%
	ΔR_c	0.26%	2.85%	0.47%	3.48%	0.27%	0.89%

TABLE 6. Results comparison between MCDPSO and ANSYS simulations.

Methods	Number	1	2	3	4	5	6	7	8
Results obtained by MCDPSO	$\max(F_{in})$/N	0.3180	0.3240	0.3270	0.3320	0.3370	0.3400	0.3450	0.3520
	$R_c^{F_{in}=\max(F_{in})}$ / mΩ	1.530	1.520	1.510	1.500	1.490	1.480	1.470	1.460
Results obtained by ANSYS simulation	$\max(F_{in})$/N	0.3457	0.3480	0.3490	0.3650	0.3613	0.3690	0.3857	0.3989
	$R_c^{F_{in}=\max(F_{in})}$ / mΩ	1.572	1.566	1.503	1.528	1.508	1.486	1.511	1.465
Differences between the two methods	ΔF_{in}	8.01%	6.90%	6.30%	9.04%	6.73%	7.86%	10.55%	11.76%
	ΔR_c	2.67%	2.94%	0.47%	1.83%	1.19%	0.40%	2.71%	0.34%

TABLE 7. Average differences between multi-objective methods and ANSYS Simulations.

Objective	$\overline{\Delta F_{in}}$	$\overline{\Delta R_c}$
MOPSO vs ANSYS	9.63%	1.37%
MCDPSO vs ANSYS	8.39%	1.57%

practical significance. The ANSYS simulation results verify the feasibility of the multi-objective optimization methods. And the calculation time of multi-objective optimization methods is far less than the ANSYS simulation. In summary, multi-objective optimization methods are more efficient than ANSYS simulation. The comparison between MCDPSO and MOPSO has been analyzed in the previous subsection.

V. CONCLUSION

The design of the optimal structure parameters for a high-speed backplane connector contact pair, originally conceived with classic schemes such as the quadrature method, was obtained using multi-objective optimization strategies. The insertion force and contact resistance of the contact pair were obtained by analyzing its mating process. The optimization model was based on the minimum insertion force during the insertion process and minimum resulting contact resistance. MCDPSO, an improved multi-objective particle swarm optimization algorithm with higher efficiency, in consideration of Pareto domination and crowding distance, was proposed to solve this engineering problem. Dynamic inertial weighting was used to balance the algorithm's search ability. External archive updates and *gbest* selection strategies were employed to improve the diversity of the non-dominated solutions relative to MOPSO. MCDPSO produced a few optimal solutions that can provide guidance for subsequent optimization designs. Compared to the original design, both the insertion force and the contact resistance of the optimal solutions were reduced. The results of multi-objective numerical methods were well verified via ANSYS simulation from the perspective of the mechanical structure.

ACKNOWLEDGMENT

The authors would also like to acknowledge the anonymous reviewers for their valuable comments and suggestions that helped to improve the quality of the paper.

REFERENCES

[1] W.-F. Leong and G. G. Yen, "Dynamic population size in PSO-based multiobjective optimization," in *Proc. IEEE Int. Conf. Evol. Comput.*, Jul. 2006 pp. 1718–1725.

[2] H. W. Johnson, "High-speed backplane connectors," in *Proc. IEEE Int. Symp. Electromagn. Compat.*, Aug. 2011, pp. 612–618.

[3] B. Hult, "Trends in high-speed backplane connectors," *Connector Specifier*, vol. 21, no. 11, pp. 15–16, Nov. 2005. [Online]. Available: http://apps.webofknowledge.com/full_record.do?product=UA&search_mode=GeneralSearch&qid=1&SID=7D11IEqDMYqn7JJSlGo&page=1&doc=1

[4] G.-P. Luo, J.-G. Lu, and J.-G. Zhang, "Failure analysis on bolt-type power connector's application," in *Proc. 45th IEEE Holm Conf. Elect. Contacts*, Oct. 1999, pp. 77–86.

[5] Z. Zeng, X. Li, M. Li, B. Huang, R. Wang, and C. Xia, "Analysis of power consumption on laser solder joints of electric connector," *Chin. J. Electron.*, vol. 23, no. 4, pp. 666–668, 2014.

[6] Z. Zeng, X. Li, R. Wang, and M. Li, "Numerical modeling and optimization of laser soldering for Micro-USB electric connector," *Int. J. Numer. Model. Electron. Netw. Devices Fields*, vol. 28, no. 2, pp. 175–188, 2015.
[7] B. Huang, X. Li, Z. Zeng, and N. Chen, "Mechanical behavior and fatigue life estimation on fretting wear for micro-rectangular electrical connector," *Microelectron. Rel.*, vol. 66, pp. 106–112, Nov. 2016.
[8] A. El Manfalouti, N. Benjemaa, and R. El Abdi, "Experimental and analytical models of the connector insertion-extraction phase," in *Proc. 50th IEEE Holm Conf. Elect. Contacts, 22nd Int. Conf. Elect. Contacts*, Sep. 2004, pp. 320–325.
[9] A. El Manfalouti, N. Benjemaa, and R. El Abdi, "Experimental and analytical models of the connector inserti on-extraction phase," in *Proc. 50th IEEE Holm Conf. Elect. Contacts, 22nd Int. Conf. Elect. Contacts*, Sep. 2004, pp. 751–758.
[10] A. Beloufa, N. E. Mastorakis, and O. Martin, "Influence of shapes, contact forces and high copper alloys on the contact resistance and temperature," in *Proc. Math. Comput. Sci. Eng. WSEAS Int. Conf.*, 2009, pp. 139–144.
[11] Z. Zeng, Z. Zhou, X. Li, M. Tang, and B. Peng, "Numerical modeling and optimization on micro-D electrical connector," *Int. J. Numer. Model.-Electron. Netw. Devices Fields*, vol. 31, no. 1, p. e2256, Jan./Feb. 2018.
[12] Y. Li, F. Zhu, Y. Chen, K. Duan, K. Tang, and S. Liu, "Analysis of insertion force of electric connector based on FEM," in *Proc. 21th Int. Symp. Phys. Failure Anal. Integr. Circuits*, Jun./Jul. 2014, pp. 195–198.
[13] A. El Manfalouti, N. B. Jemaa, and E. Rochdi, "A new experimental method for the determination of connector parameters in insertion and extraction phase," *IEICE Trans. Electron.*, vol. E87-C, no. 8, pp. 1289–1294, 2004.
[14] Y.-L. Hsu, Y.-C. Hsu, and M.-S. Hsu, "Shape optimal design of contact springs of electronic connectors," *J. Electron. Packag.*, vol. 124, no. 3, pp. 178–183, 2002.
[15] S. Fallahian, D. Hamidian, and S. M. Seyedpoor, "Optimal design of structures using the simultaneous perturbation stochastic approximation algorithm," *Int. J. Comput. Methods*, vol. 6, no. 2, pp. 229–245, 2009.
[16] M. E. Lotfy, T. Senjyu, M. A. Farahat, A. F. Abdel-Gawad, and A. Yona, "Enhancement of a small power system performance using multi-objective optimization," *IEEE Access*, vol. 5, pp. 6212–6224, 2017.
[17] R. Liu, R. Wang, W. Feng, J. Huang, and L. Jiao, "Interactive reference region based multi-objective evolutionary algorithm through decomposition," *IEEE Access*, vol. 4, pp. 7331–7346, 2016.
[18] B. Cao *et al.*, "Distributed parallel particle swarm optimization for multi-objective and many-objective large-scale optimization," *IEEE Access*, vol. 5, pp. 8214–8221, 2017.
[19] H. M. Alsaket, K. R. Mahmoud, H. M. Elattar, and M. A. Aboul-Dahab, "Exploring evolutionary multi-objective techniques in self-organizing networks," *IEEE Access*, vol. 5, pp. 12049–12060, 2017.
[20] W. Yu, X. Li, H. Yang, and B. Huang, "A multi-objective metaheuristics study on solving constrained relay node deployment problem in WSNS," *Intell. Automat. Soft Comput.*, vol. 24, no. 2, pp. 367–376, 2018.
[21] Y. Zhang, D.-W. Gong, and Z. Ding, "A bare-bones multi-objective particle swarm optimization algorithm for environmental/economic dispatch," *Inf. Sci.*, vol. 192, pp. 213–227, Jun. 2012.
[22] L. Li, W. Wang, and X. Xu, "Multi-objective particle swarm optimization based on global margin ranking," *Inf. Sci.*, vol. 375, pp. 30–47, Jan. 2017.
[23] Y. Zhang, D.-W. Gong, J.-Y. Sun, and B.-Y. Qu, "A decomposition-based archiving approach for multi-objective evolutionary optimization," *Inf. Sci.*, vols. 430–431, pp. 397–413, Mar. 2018.
[24] A. M. El-Zonkoly, "Optimal placement of multi-distributed generation units including different load models using particle swarm optimization," *Swarm Evol. Comput.*, vol. 1, no. 1, pp. 50–59, 2011.
[25] T. Navalertporn and N. V. Afzulpurkar, "Optimization of tile manufacturing process using particle swarm optimization," *Swarm Evol. Comput.*, vol. 1, no. 2, pp. 97–109, 2011.
[26] M. A. Ahandani, M. T. V. Baghmisheh, M. A. B. Zadeh, and S. Ghaemi, "Hybrid particle swarm optimization transplanted into a hyper-heuristic structure for solving examination timetabling problem," *Swarm Evol. Comput.*, vol. 7, pp. 21–34, Dec. 2012.
[27] A. A. Mousa, M. A. El-Shorbagy, and W. F. Abd-El-Wahed, "Local search based hybrid particle swarm optimization algorithm for multiobjective optimization," *Swarm Evol. Comput.*, vol. 3, pp. 1–14, Apr. 2012.
[28] N. C. Sahoo, S. Ganguly, and D. Das, "Multi-objective planning of electrical distribution systems incorporating sectionalizing switches and tie-lines using particle swarm optimization," *Swarm Evol. Comput.*, vol. 3, pp. 15–32, Apr. 2012.
[29] S. Tyagi and K. K. Bharadwaj, "Enhancing collaborative filtering recommendations by utilizing multi-objective particle swarm optimization embedded association rule mining," *Swarm Evol. Comput.*, vol. 13, pp. 1–12, Dec. 2013.
[30] S. Cheng, M.-Y. Chen, and P. J. Fleming, "Improved multi-objective particle swarm optimization with preference strategy for optimal DG integration into the distribution system," *Neurocomputing*, vol. 148, pp. 23–29, Jan. 2015.
[31] M. J. Mahmoodabadi, M. B. S. Mottaghi, and A. Mahmodinejad, "Optimum design of fuzzy controllers for nonlinear systems using multi-objective particle swarm optimization," *J. Vib. Control*, vol. 22, no. 3, pp. 769–783, 2016.
[32] S. Timsit, "Electrical contact resistance: Properties of stationary interfaces," in *Proc. 44th IEEE Holm Conf. Elect. Contacts*, Oct. 1998, pp. 1–19.
[33] R. Holm, *Electric Contacts: Theory and Application*. Berlin, Germany: Springer-Verlog, 2013.
[34] G. Abbas, J. Gu, U. Farooq, M. U. Asad, and M. El-Hawary, "Solution of an economic dispatch problem through particle swarm optimization: A detailed survey—Part I," *IEEE Access*, vol. 5, pp. 15105–15141, 2017.
[35] M. Reyes-Sierra and C. A. Coello, "Multi-objective particle swarm optimizers: A survey of the state-of-the-art," *Int. J. Comput. Intell. Res.*, vol. 2, no. 3, pp. 287–308, 2006.
[36] T. Huang and A. S. Mohan, "A hybrid boundary condition for robust particle swarm optimization," *IEEE Antennas Wireless Propag. Lett.*, vol. 4, pp. 112–117, 2005.
[37] A. Lipowski and D. Lipowska, "Roulette-wheel selection via stochastic acceptance," *Phys. A, Statist. Mech. Appl.*, vol. 391, no. 6, pp. 2193–2196, 2012.
[38] K. Deb, A. Pratap, S. Agarwal, and T. Meyarivan, "A fast and elitist multiobjective genetic algorithm: NSGA-II," *IEEE Trans. Evol. Comput.*, vol. 6, no. 2, pp. 182–197, Apr. 2002.
[39] J. E. Alvarez-Benitez, R. M. Everson, and J. E. Fieldsend, "A MOPSO algorithm based exclusively on pareto dominance concepts," in *Proc. Int. Conf. Evol. Multi-Criterion Optim.*, vol. 3410. Berlin, Germany: Springer, 2005, pp. 459–473.
[40] C. A. C. Coello and M. S. Lechuga, "MOPSO: A proposal for multiple objective particle swarm optimization," in *Proc. Congr. Evol. Comput., IEEE World Congr. Comput. Intell.*, May 2002, pp. 1051–1056.
[41] E. Zitzler and L. Thiele, "Multiobjective evolutionary algorithms: A comparative case study and the strength Pareto approach," *IEEE Trans. Evol. Comput.*, vol. 3, no. 4, pp. 257–271, Nov. 1999.
[42] J. R. Schott, "Fault tolerant design using single and multicriteria genetic algorithm optimization," Air Force Inst. Technol., Wright-Patterson AFB, OH, USA, Tech. Rep. AFIT/CI/CIA-95-039, 1995.
[43] Y. Shi and R. Eberhart, "A modified particle swarm optimizer," in *Proc. IEEE Int. Conf. Evol. Comput.*, May 1998, pp. 69–73.
[44] R. E. Perez and K. Behdinan, "Particle swarm approach for structural design optimization," *Comput. Struct.*, vol. 85, nos. 19–20, pp. 1579–1588, Oct. 2007.
[45] Y. Jiang, T. Hu, C. Huang, and X. Wu, "An improved particle swarm optimization algorithm," *Appl. Math. Comput.*, vol. 193, no. 1, pp. 231–239, Oct. 2007.

WENJIE YU received the M.S. and Ph.D. degrees in mechanical engineering from the University of Electronic Science and Technology of China in 2013 and 2017, respectively. Currently, he is doing a two-year post-doctoral at the University of Electronic Science and Technology of China. His current research interests include wireless sensor networks, multi-objective optimization, and swarm intelligence.

ZHI ZENG received B.S., M.S., and Ph.D. degrees in materials science and engineering in 2004, 2006, and 2009, respectively. He is currently an Associate Professor with the Department of Mechatronics Engineering, University of Electronic Science and Technology of China. His research activities have been concerned with laser soldering, welding, modeling, and simulation in materials science and engineering.

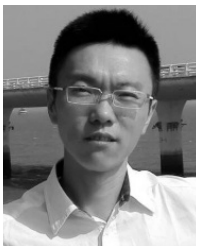

BEI PENG received the B.S., two M.S., and Ph.D. degrees in mechanical engineering in 1999, 2000, 2003, and 2008, respectively. He is currently a Professor with the Department of Mechatronics Engineering, University of Electronic Science and Technology of China. His current research interests include micro-electromechanical systems, robot technology, sensor technology, and intelligent manufacturing technology.

SHUO YAN is currently pursuing the M.S. degree in mechanical engineering with the University of Electronic Science and Technology of China. His research interests include mechanical modeling and 3-D printing.

YUESHUANG HUANG is currently pursuing the M.S. degree in mechanical engineering with the University of Electronic Science and Technology of China. His research interests include swarm intelligence and 3-D printing.

HAI JIANG received the B.S. and M.S. degrees from Chongqing University, and the Ph.D. degree from the University of Waterloo, all in mechanical engineering. He is currently an Associate Professor with the Department of Mechatronics Engineering, University of Electronic Science and Technology of China. His current research interests include microfluidic technology and intelligent manufacturing technology.

XUNBO LI received the M.S. degree in machinery and the Ph.D. degree in measurement and instrument from the University of Electronic Science and Technology of China in 1991 and 2001, respectively. Currently, he is a Professor at the School of Mechatronics Engineering, University of Electronic Science and Technology of China, and the Director of the Institute of Electrical and Mechanical Intelligent Control. His current research interests include intelligent measurement and control technology research and the applications of mechanical and electrical.

TAO FAN received the B.S. and M.S. degrees in mechatronics engineering from the University of Electronic Science and Technology of China in 2014 and 2017, respectively. His research interests include mechanical modeling and swarm intelligence.